Studia Geotechnica et Mechanica, 2020; 42(3): 210–221

Original Study

Open Access

Abdelaziz Khennouf*, Mohamed Baheddi

# Heave analysis of shallow foundations founded in swelling clayey soil at N'Gaous city in Algeria

https://doi.org/10.2478/sgem-2019-0051
received September 9, 2019; accepted May 14, 2020.

**Abstract:** The design of shallow foundations on swelling soils needs a thorough study to evaluate the effect of swelling potential soil on the final foundation heave. For this reason, a simple analytical approach based on the soil stress state under the foundation can be used to calculate the foundation heave. This paper reports a set of analytical and numerical analysis using the finite-difference code (FLAC 3D), performed on an isolated shallow foundation founded on a swelling soil mass at N'Gaous city in Batna Province, Algeria, subjected to distributed vertical loads. Further, the influence of some parameters on total heave was analyzed, such as the embedded foundation and soil stiffness. The analysis results from the proposed 3D modelling was compared and discussed with analytical results. The numerical results obtained show a good agreement with the analytical solutions based on oedometer tests proposed in the literature, and deliver a satisfactory prediction of the heave of the shallow foundations.

**Keywords:** Clayey soils; swelling; analytical approach; foundation heave; numerical modelling.

## 1 Introduction

A swelling soil is generally defined as a soil that has a potential to increase in volume under increasing water content.[1,2] Clay soils consist of various minerals with a high affinity for water such as kaolinite, illite and montmorillonite. Moreover, the mechanism of hydration from a certain state induces significant swelling, especially montmorillonite mineral, which has most of the problems of swelling soils.[3] Swelling soils are found in many parts of the world, particularly in arid and semi-arid areas, where moist conditions happen after long periods of desiccation. In the literature, several studies have been conducted on problems related to swelling soils, for example, Nelson and Miller,[1] Nelson et al.,[2] Chen,[3] Fredlund et al.[4]

The high swelling pressure, causes differential structures' heaving, in particular light structures of low stiffness built on shallow foundations.[5] However, this heaving induces costly damage, most of which is cracks in walls and slabs. Algeria, like other countries with a dry climate, also suffers from the problem of soil swelling. Several cases of damages have occurred in recent years in many parts of the country (e.g., Medea, Batna, Tlemcen, Oran).[6–8]

Soil-structure interaction is assured by the foundations, which have the important role of transferring loads to the supporting soils. For this reason, when studying the foundation swelling soils of a construction, should interest with their mechanical behavior under the applied loads, also take into account that swelling strain of clay soils occur over time as a function of soil properties[9] (e.g., mineralogy, structure, suction, plasticity and dry density, permeability), also the environmental conditions (e.g., moisture variations, climate, vegetation).[10]

Many researchers have developed expressions to calculate the total heave on an unsaturated swelling soil by taking into account the soil suction, for example, Mitchell and Avalle,[11] Mckeen,[12] Fityus and Smith,[13] Briaud et al.,[14] Vanapalli et al.[15] Moreover, expressions for saturated swelling soil based on oedometer tests have been reported in literature, for example, Fredlund,[16] US Department of the army,[17] Nelson et al.,[18] Ejjaaouani and Shakhirev,[19] Baheddi et al.,[20] where each researcher proposes an expression based on the type of swelling tests that have been performed on the oedometer.

In literature, several researchers have numerically investigated the problem of shallow foundations on unsaturated swelling soils using 2D finite element analysis, for example, Hung and Fredlund,[21,23] Masia et al.,[22] Abed,[24] Nowamooz et al.[25] So, they conducted

***Corresponding author: Abdelaziz Khennouf,** Laboratory of Natural Risk and Regional Planning (LRNAT), Department of Civil Engineering, University of Batna 2, Algeria, E-mail: a.khennouf@univ-batna2.dz
**Mohamed Baheddi,** Laboratory of Natural Risk and Regional Planning (LRNAT), Department of Civil Engineering, University of Batna 2, Algeria

a hydro-mechanical study to estimate the effect of the drying-wetting path on the shrinkage and heave of the shallow foundations. Nevertheless, few studies are found providing a detailed behavior of shallow foundations on swelling soils using 3-D numerical modelling. This is due to the lack of a particular behavior model of swelling soil in recent years. Therefore, this complexity along the soil behavior, has encouraged the use of a simple method for modeling swelling soil in the present study. This method based on the simulation of swelling pressure in vertical direction of all soil mass.

In this study, isolated shallow foundations such as square, rectangular and circular footing were analyzed due to the limited study of their mechanical behavior in swelling soil by researchers. In addition, the majority of damaged structures with low stiffness are based on this type of shallow foundations. All these reasons made us choose 3-D numerical modeling.

A short description of geotechnical properties of the soil located at N'Gaous city in Batna Province, Algeria, of the analytical approach according to the soil stress state and the equations used for predicting total heave based on oedometer test is presented. A three-dimensional numerical model using the finite difference code FLAC was used to analyze the total heave. The numerical results obtained were compared with the analytical results proposed in the literature.

## 2 Properties of the swelling clay

The studied swelling clay is located in N'Gaous city near Hospital (35° 34' 04.8" N, 5° 36' 60.0" E), which is located 77 km west of Batna Province, Algeria. Most part of this region is recognized by the abundance of active soils and the damage related to the light structure, as in Fig. 1. Table 1 summarizes the physical and mechanical properties of the undisturbed soil samples taken in the present study.

The soil was classified as a highly plastic silty clay (CH), in accordance with the Unified Soil Classification System (USCS). The experimental results using the conventional one-dimensional oedometer according to ASTM standard D 4546-08[26] produced various curves giving the swelling strain versus time (see Fig. 2), which shows the free swelling strain. As well as the swelling strain as a function of vertical pressure, which shows the swelling pressure for a null swelling strain (see Fig. 3). Following this method, a single-undisturbed sample was loaded at a very low stress level $\sigma_i$=1 kPa, the soil was wetted and allowed to swell, until swelling ceases. This vertical swell was registered as the free swelling strain. After that, the vertical pressure was then applied in increments to gradually consolidate the soil sample. The pressure required to consolidate the soil sample to its initial volume ($\varepsilon_{sw}$=0 %) is defined as a swelling pressure. The free swelling strain and swelling pressure were 8.86% and 218 kPa, respectively, as shown the curve in Figure 2 and Figure 3.

**Table 1:** Geotechnical characteristics of soil samples.

| **Soil properties** | **Value** |
|---|---|
| Sampling depth | 2.3–2.5 m |
| Liquid limit, ***LL*** (%) | 72.28 |
| Plastic limit, ***PL*** (%) | 29.20 |
| Plasticity Index, ***PI*** (%) | 43.08 |
| Natural dry unit weight, $\gamma_d$ (**kN/m³**) | 17.5 |
| Natural wet unit weight, $\gamma_h$ (**kN/m³**) | 20.0 |
| Specific Gravity, $G_s$ | 2.74 |
| Natural water content, $W_n$ (%) | 14.1 |
| Natural degree of saturation, $S_r$ (%) | 80.82 |
| Initial void ratio, $e_0$ | 0.478 |
| Compression Index, $C_c$ | 0.15 |
| Swelling Index, $C_s$ | 0.054 |
| Preconsolidation pressure, $P_c$ **(kPa)** | 190 |
| Cohesion, after saturation ***C*** **(kPa)** | 100 |
| Friction angle, after saturation $\varphi$ (°) | 25 |
| Grain size distribution | 71 |
| Clay (%) | 24.5 |
| Silt (%) | 4.5 |
| Sand (%) | 98.90 |
| C80 µm (%) | 71 |
| C2 µm (%) | |

## 3 Analytical approaches

In the calculation of the total heave of shallow foundations after soil swelling, it is necessary to consider the soil stress state under the foundation as well as the swelling pressure. The soil stress state is determined by the calculation of two stress components, mentioned as follows: the geostatic stresses $\sigma_{z,g}$, which are increasing linearly with depth and can be computed using the classic equation $\sigma_{z,g}=\gamma_{sw}\times z$. The loading stresses $\sigma_{z,load}$ are due to the construction weight, decrease with depth[27] and can be computed using Equation (1).[28] In addition, this simple approach is generally related to the foundation found on a horizontal surface and homogeneous soil.

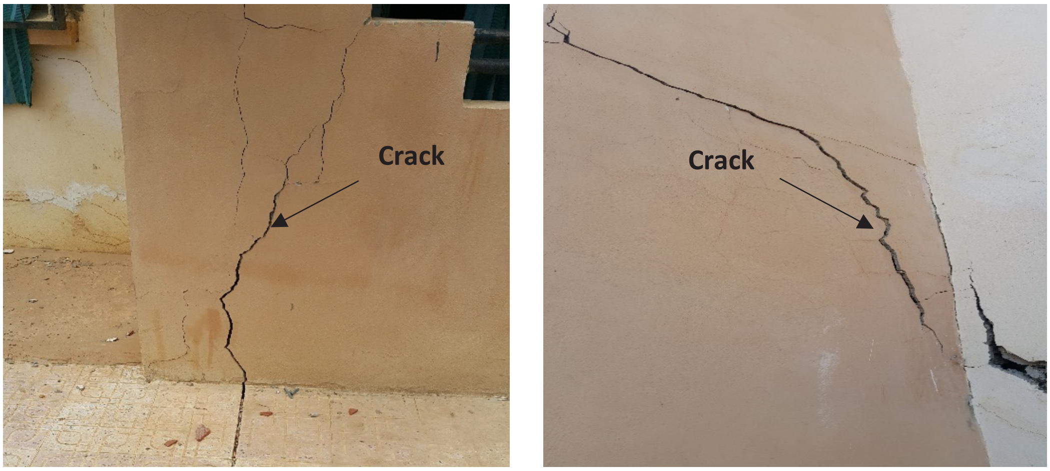


**Figure 1:** Example of damage of swelling soil in N'Gaous city.

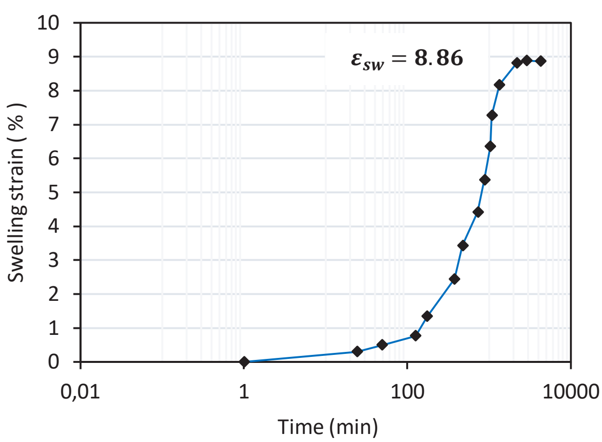


**Figure 2:** Free swelling strain versus elapsed time.

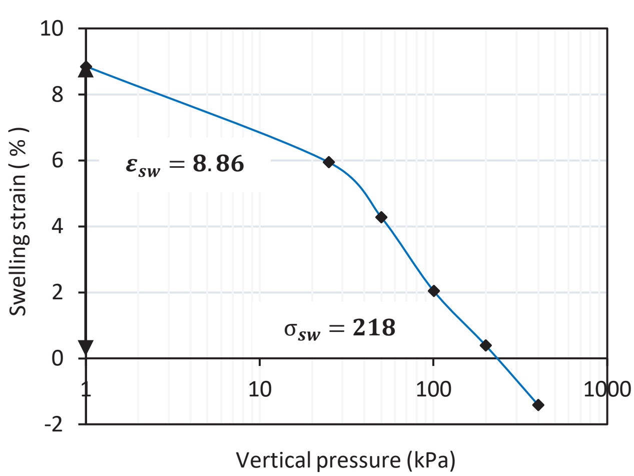


**Figure 3:** Swelling strain versus vertical pressure

$$\sigma_{z,load} = \frac{\sigma_0 . B . L}{(B+Z)(L+Z)} \tag{1}$$

where $\sigma_0$ is the distributed load applied at the foundation level; $B$ is the width of the foundation; $L$ is the length of the foundation and $z$ is the depth considered below the foundation level.

Baheddi et al.[20] determined that the vertical swelling strain of saturated soils occurs in the boundaries of the swelling zone II (see Fig. 4), where the total stress $\sigma_{z,t}$ is less than the swelling pressure $\sigma_{sw}$ as indicated by the Equation (2):

$$\sigma_{z,t} = \sigma_{z,g} + \sigma_{z,load} < \sigma_{sw} \tag{2}$$

## 3.1 Prediction of total heave

In the late 1950s, heave prediction methods were first developed as extensions of methods used to estimate volume changes due to consolidation in saturated soils using results of one-dimensional oedometer (consolidation) tests.[2,29]

There are several methods to measure the swelling pressure by oedometer tests for swelling soils according to ASTM standard D 4546-08,[26] among which is the constant volume (CV) method. The swell-consolidation (CS) method and loaded swell (LS) method, which need many identical samples, have also been used.[30–32] The swell and swelling pressure determined from these tests are the main parameters used to compute the total heave. The total heave of the homogeneous soil profile $S_{sw}$ is equal to the sum of the increments heaving $\Delta h_i$ for each elementary layer $h_i$, as shown in Figure 5. So, it is necessary to take into account in calculation the total stress variation $\sigma_{zi,t}$ in the middle of each elementary layer under the center of the foundation.

The depth at which the swelling pressure equals the total geostatic stress is defined as the depth of potential heave $H$, as indicated by Equation (3),[33] this depth represents the maximum depth of the active zone.

$$\gamma_{sw} \times H = \sigma_{sw} \tag{3}$$

In the case of shallow foundations founded in a swelling soil, the depth of potential heave $H$ is determined in free-field; after that, loading stresses $\sigma_{z,load}$ transmitted by the foundation are added to the total stress $\sigma_{z,t}$ for computation of foundation heave. This was used in analytical calculations.

In this study, the clayey soil is assumed to be homogeneous. The depth of potential heave ($H= \sigma_{sw}/\gamma_{sat}$) equals 11 m for $\sigma_{sw}$ = 218 kPa and $\gamma_{sat}$ = 20 KN/m$^3$, which was obtained experimentally, whereas the depth was divided into equal layers $h_i$=1m for all the analytical calculations. It would be preferable to choose a layer thickness as small as possible to increase the accuracy of the calculations.[2] Two equations were used in the present work for predicting the total heave based on swell-consolidation (CS) test.

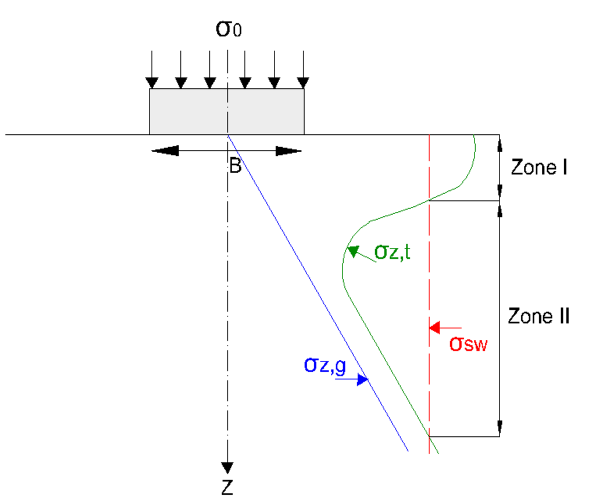


**Figure 4:** Scheme of stresses distributions in the soil below a shallow foundation.

### 3.1.1 Department of the Army

Technical Manual by the US Department of the Army[17] proposed Equation (4) for the prediction of total heave:

$$S_{sw} = \sum_{i=1}^{n} \Delta h_i = \sum_{i=1}^{n} \left\{ C_{DA} h \log\left[\frac{\sigma_{cs}}{\sigma_f}\right]\right\}_i \tag{4}$$

where $S_{sw}$ is the total heave; $\Delta h_i$ is the heave of layer $i$; $h$ is the initial thickness of layer $i$; $C_{DA}$ is the Department of Army heave parameter determined from the slope of the swelling strain versus pressure curve in Figure 3 ($C_{DA} = \varepsilon_{sw}/\log(\sigma_{cs}/\sigma_i)$) ; $\sigma_i$ is the initial pressure from CS test of layer $i$; $\sigma_{cs}$ is the swelling pressure from CS test of layer $i$ and $\sigma_f$ is the final vertical normal stress of layer $i$ ($\sigma_f=\sigma_{z,t}= \sigma_{z,g}+\sigma_{z,load}$).

The obtained value is: $C_{DA}$ = 0.0886/log(218/1 ) = 0.037.

### 3.1.2 Nelson and Miller

Nelson and Miller[1] proposed Equation (5) for the prediction of total heave:

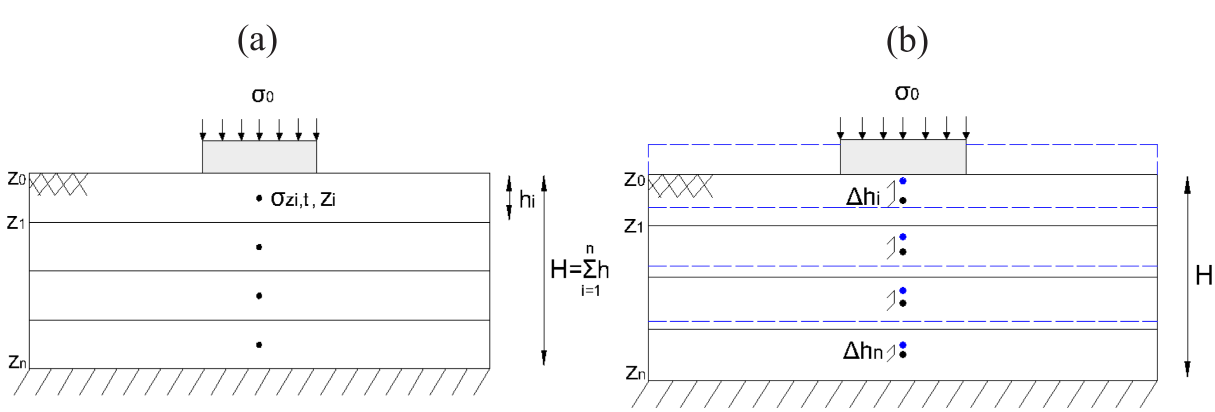


**Figure 5:** (a) Initial states of layers, (b) Final states of layers after total heave.

$$S_{sw} = \sum_{i=1}^{n} \Delta h_i = \sum_{i=1}^{n} \left\{ \frac{C_s}{1+e} h \log \left[ \frac{\sigma_{cs}}{\sigma_f} \right] \right\}_i \tag{5}$$

where $C_s$ is the swelling index of layer $i$ and $e$ is the initial void ratio of layer $i$.

The used values are: $C_s$ = 0.054 and $e$ = 0.478.

# 4 Numerical modelling approach

In this study, analytical solutions can be sufficient to determine the total heave. However, the key limitation of these solutions is that the heave is only given in the center of the footing. So, numerical modelling is necessary because it allows to determine the final state of the soil and foundations after the swelling and to study the influence of several factors such as soil properties and geometric characteristics of foundations as well.

Numerical study was performed using the finite difference method FLAC 3D.[34] A large number of calculation steps were used in the explicit Lagrangian resolution scheme. The maximum unbalanced force is the magnitude of the vector sum of the nodal forces for all the nodes within the mesh. When the maximum unbalanced force is small compared with the total applied force associated with stress or boundary displacement changes, the model is considered to be in equilibrium. The failure and plastic flow phenomena occur within the model when the unbalanced force approaches a constant value.

A rigid square shallow foundation of width $B$=1 m and thickness of 0.2 m was considered. This foundation was located at the surface of the swelling clayey soil and subjected to a distributed vertical loading $\sigma_0$ varying from 0 to 500 kPa. Because of the symmetrical nature of the problem and in order to reduce computation time, only a quarter of the system was modeled, as shown in Figure 6. The model was extended in both horizontal directions $L_x$=15 m, $L_y$=15 m and a total height $H$=11 m. For boundary conditions, the base of the model was constrained in all directions and the horizontal displacement was zero in the $x$-direction for the planes $x$=0 and $x$=15. Similarly, there was no displacement in $y$-direction for the planes $y$=0 and $y$=15.

The rigid square footing was made of concrete, modeled by a group of brick elements with a linear elastic constitutive model. The elastic moduli used were the shear modulus $G$=12.5 GPa and the bulk modulus $K$=16.67 GPa (equivalent to Young's modulus $E$=30 GPa and a Poisson's ratio $\nu$=0.2) and the unit weight $\gamma$=25 KN/

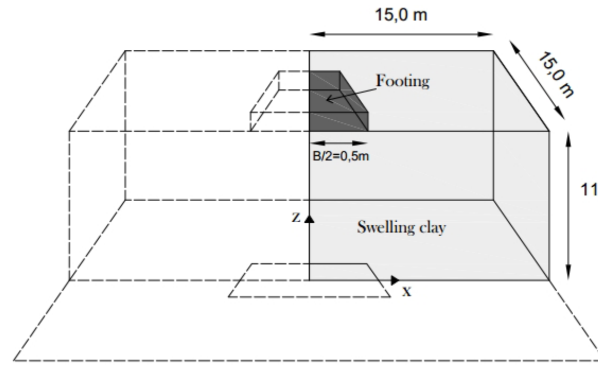


**Figure 6:** Geometry of the model.

m³. It is important to note that if the footing is rigid, the parameters of concrete don't influence the solution. The swelling clay is modelled using a linear elastic–perfectly plastic constitutive model following the Mohr–Coulomb (MC) failure criterion. The Mohr-Coulomb model is widely used in numerical modelling in geotechnical engineering due to its simplicity and accuracy. This model involves five parameters: the elastic modulus $E$, the Poisson's ratio $\nu$, the cohesion $C$, the internal friction angle $\varphi$ and the dilatancy angle $\psi$. Table 2 provides the model parameters used in the simulation. The elastic modulus $E$, which is used in the present study was conventionally estimated from the oedometer modulus $E_{oed}$ and the Poisson's ratio $\nu$. According to Hook's law, the relationship is given using Equation (6)[35]:

$$E = E_{oed} \frac{(1-2\nu)(1+\nu)}{(1-\nu)} \tag{6}$$

where the Poisson's ratio $\nu$ is constant and was estimated from the at rest earth pressure coefficient $K_0$ using Equation (7).[11]

$$\nu = \frac{K_0}{1+K_0} \tag{7}$$

The effective stiffness parameters represented by elastic modulus and Poisson's ratio of the soil are 10 MPa and 0.35, respectively. These two parameters are mainly affecting the evolution of soil heave.[21] However, the strength parameters represented by the cohesion and the internal friction angle are 100 kPa and 25°, respectively. These parameters were obtained from drained direct shear tests performed on soil samples after saturation.

**Table 2:** Soils parameters used in the numerical study.

| Parameters | Value |
|---|---|
| Unit weight, $\gamma$ (kN/m$^3$) | 20 |
| Elastic Modulus, $E$ (MPa) | 10 |
| Poisson's ratio, $v$ | 0.35 |
| Cohesion, $C$ (kPa) | 100 |
| Friction angle, $\varphi$ (°) | 25 |
| Dilatancy angle, $\psi$ (°) | 0 |

Note: $k = \frac{E}{3(1-2v)}$ ; $G = \frac{E}{2(1+v)}$

The discretization of the model was made by primitive elements of brick form with a local refinement of the most stressed and deformed zone, that is, in the vicinity and at the base of the footing. Many of the mesh sensitivity tests have been performed to ensure that the mesh size has no impact on the numerical results and to find the optimal mesh size. The optimal mesh size allows the modeler to spend less time in calculation. In all cases, an identical mesh size between the footing and the soil is well-defined to ensure connectivity of the nodes at the interface soil-footing. The mesh size was limited as 0.05 B to the footing surface and near the footing edge. Therefore, the number of footing elements was 100 and the mesh consisted entirely of 36850 elements and 40297 nodes, as shown in Figure 7.

The rigid footing was in contact with the soil through the interface element using the Mohr-Coulomb failure criterion. A rough interface along the base of the footing was adopted that had a cohesion $C_{int}$=100 kPa and a friction angle $\varphi_{int}$=25°, and also a normal stiffness $K_n$=$10^8$ Pa/m and shear stiffness $K_s$=$10^8$ Pa/m. According to Itasca,[33] a good rule-of-thumb is that $K_n$ and $K_s$ be set to ten times the equivalent stiffness of the stiffest neighboring zone. The apparent stiffness of a zone in the normal direction is:

$$max\left[\frac{K+\frac{4}{3}G}{\Delta z_{min}}\right] \tag{8}$$

where $K$ and $G$ are the bulk and shear moduli, respectively; $\Delta z_{min}$ is the smallest width of an adjoining zone in the normal direction.

Swelling soil was modeled in the initial state by the simulation of swelling pressure. In this phase, the model was subjected to gravitational loading, then to a vertical swelling pressure that equals 218 kPa constant throughout the entire depth was applied. During this phase, the model was monitored to ensure that no plastic points occur. After that, initial horizontal stresses were generated using $K_0$ equal 0.57. This ensures that horizontal stresses have been generated associated with the swelling pressure. The simulation steps included generating an initial stress condition, an interface and a footing activation followed by several compressing loading steps $\sigma_0$ applied on the footing.

The load was applied to the footing with a uniform pressure surface. The choice of this type of loading gives a good comparison with the simulated swelling pressure, which is uniformly distributed. During the modelling, the vertical displacement (heave) was followed until a constant value was reached at the end of loading. In this study, the ratio of the maximum unbalanced force taken was equal to $10^{-5}$. This ratio is recommended by Itasca to achieve equilibrium.

# 5 Results and Discussion

## 5.1 Foundation heave-model validation

Figure 8 shows heave $S_{sw}$ obtained by the analytical and numerical approaches at the center of foundation for various vertical loads $\sigma_0$. The results obtained indicated that there was a non-linear decrease in heaving with the load's increase on the footing. However, by comparing the analytical results with the numerical ones that were obtained using FLAC software. The total heave predicted in the numerical study showed an excellent agreement with the analytical results of the Department of the Army[17] and Nelson and Miller,[1] within a percentage difference of approximately 2%, for example, for total heaving at the last loading $\sigma_0$=500 kPa based on the analytical output of the Department of the Army along with Nelson and Miller, $S_{sw}$=78.28 mm and $S_{sw}$=75.49 mm were observed, respectively, and the numerical analysis showed $S_{sw}$=81 mm. Therefore, the results showed a reasonable capability and efficiency of the proposed numerical model to predict the heave of the footing under vertical loading.

An important implication of these findings was that the footing continued to heave when the load exceeded the swelling pressure 218 kPa; this explained the appearance of a localized settlement of the upper layers of soil that was under the foundation, where the total stresses $\sigma_{z,t}$ was greater than the swelling pressure. However, beyond a certain depth, the diffusion of loading stresses can cause the total stress to be less than the swelling pressure. In this case, the lower layers of the soil would swell and the foundation would be heaving in overall and this agrees well with the analytical approach.

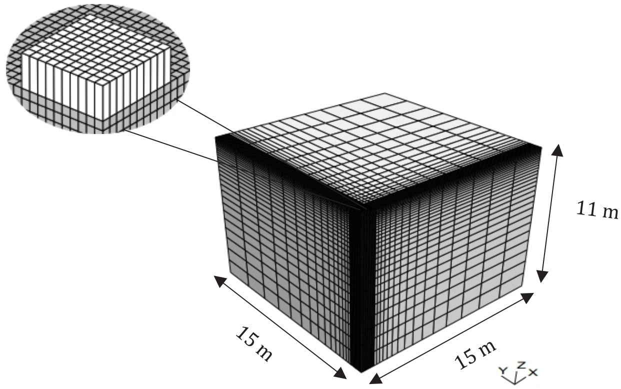


**Figure 7:** Three-dimensional mesh of the numerical model.

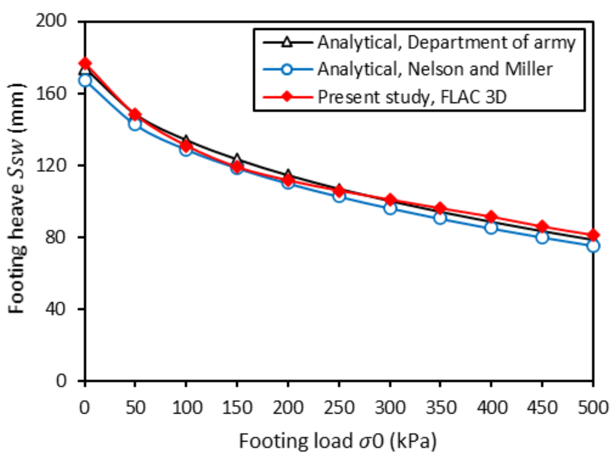


**Figure 8:** Comparison of heave results $S_{sw}$ for square footing obtained from numerical and analytical prediction.

Figure 9 illustrates contours and vectors heaving of the foundation after the applied load $\sigma_0$=100 kPa. It could be seen that a differential heave of the foundation was observed at the end of loading. Also, the heave was minimum at the center of the foundation (130.85 mm) and it attained a maximum value at the corner (148 mm). This was because the loading stress distributes its maximum value directly under the center of the footing and decreases from the outward center.

Table 3 summarizes the analytical results for total heave prediction $S_{sw}$ of the Department of the Army,[17] Nelson and Miller[1] and the present numerical results, for different types of isolated shallow foundations (rectangular and circular footing), subjected to varied loads $\sigma_0$ from 0 to 500 kPa in 100 kPa increments. Comparing the obtained results, the numerical predictions for rectangular and circular footing were in good agreement with the solutions of the Department of the Army as well as Nelson and Miller.

## 5.2 Heave evolutions throughout the soil depth

Figure 10 shows the variation of the heave $S_{sw}$ throughout the depth of the swelling soil for different load increments $\sigma_0$ obtained by the analytical results of the Department of the Army,[17] Nelson and Miller[1] as well as numerical analysis. Six curves can be identified, each one corresponding to a specific load applied to the square footing. FLAC software didn't show the displacement increments in the numerical model results. For this reason, the cumulative heave evolution along the depth could not be measured in the present numerical model and only the final heaving value was considered at the soil surface. The analytical calculation curves showed that the heave along the soil depth was non-linear. Ejjaaouani and Shakhirev[19] indicated this non-linear evolution of heaving through the soil depth. Moreover, the curves show an increase in heaving starting from the deepest point until the base of the footing. However, for loads greater than 400 kPa, the heaving is reduced when it reaches a depth of one meter below the base of the footing because of the large loading stresses in this zone. The numerical results obtained at the soil surface were compatible with the analytical results.

## 5.3 Swelling strain variation with soil thickness

Figure 11 shows the variation of vertical swelling strain of square footing $\varepsilon_{sw}$ as a function of the swelling soil layer thickness presented by $H/B$ ratio for different load increments $\sigma_0$. A variable $H/B$ ratio of 2 to 10 was used in this study ($H/B$=2;4;6;8;10). It is note that the swelling strain results was shown at the center of foundation base. The numerical results indicate that the vertical swelling strain of the footing increases along with $H/B$ ratio for all value of loads $\sigma_0$. In addition, it was observed that there was a small increase in $\varepsilon_{sw}$ for $H/B$ ratio higher than 6. However, a settlement strain found in the footing when the applied load was greater than 400 kPa at a ratio $H/B$=2.

## 5.4 Influence of the embedded footing

The influence of the square footing embedment on the total heave $S_{sw}$ was studied, the $D/B$ ratio was chosen from 0 to 1.5 in increments of 0.5 ($D/B$=0;0.5;1.0;1.5) for distributed vertical loading $\sigma_0$=100 kPa.

Figure 12 shows the variation of heave $S_{sw}$ according to $D/B$ ratio. This Figure indicates the influence of the

**Table 3:** Heave prediction for each type of isolated shallow foundations from numerical and analytical analysis.

| Foundation Type | Foundation Heave $S_{sw}$ (mm) | Applied Loads $\sigma_0$ (kPa) | | | | | |
|---|---|---|---|---|---|---|---|
| | | 0 | 100 | 200 | 300 | 400 | 500 |
| Rectangle | Calculated | | | | | | |
| B = 1 m, L = 2 m | Nelson and Miller | 167.5 | 121.3 | 98.9 | 82.42 | 68.99 | 57.48 |
| | Department of army | 173.7 | 125.79 | 102.56 | 85.47 | 71.54 | 59.61 |
| | Numerical | 158 | 125.2 | 108.9 | 96.1 | 83.7 | 71.2 |
| Circle | Calculated | | | | | | |
| D = 1.8 m | Nelson and Miller | 167.5 | 130.6 | 110.9 | 96.2 | 84.1 | 73.6 |
| | Department of army | 173.7 | 135.48 | 115.08 | 99.8 | 87.22 | 76.39 |
| | Numerical | 157.2 | 125.1 | 108.6 | 94.5 | 80.5 | 66.3 |

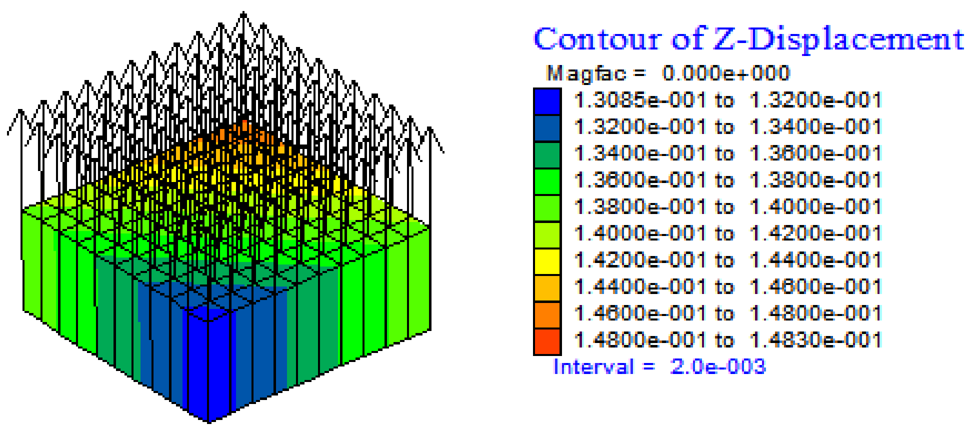


**Figure 9:** Contours and vectors heaving of square footing for $\sigma_0$=100 kPa.

footing embedment on total heave prediction, both analytically and numerically. The numerical results obtained agreed well with the analytical solution proposed by the Department of the Army[17] and Nelson and Miller,[1] with a percentage difference less than 2%. Also, the results observed showed that the heaving of the footing $S_{sw}$ decreased with an increase in the embedment ratio $D/B$. A footing embedment equal to 1.5 m resulted in a decrease of total heave around 62.70% compared to a zero embedment $D/B$=0. This significant decrease of the heave can be due to the increased effect of lateral soil friction around the footing volume, where the confining pressure at the footing edges increases its rigidity. Table 4 summarizes the analytical and numerical results of the total heave prediction for rectangular and circular footing.

## 5.5 Influence of soil stiffness

A number of numerical computations have been carried out to test the influence of soil stiffness, represented by the elastic modulus of the soil $E_{soil}$ on the final heave of the square footing $S_{sw}$ for different applied loads $\sigma_0$. The elastic modulus values were selected from 5 to 20 MPa in increments of 5 MPa ($E_{soil}$=5;10;15;20 ) in order to draw the curve showing the heave variation $S_{sw}$ as a function of the elastic modulus $E_{soil}$. The numerical results presented in Figure 13 indicated that the increase in the elastic modulus $E_{soil}$ induced a significant non-linear decrease in footing heave $S_{sw}$. Moreover, $S_{sw}$ decreased by 50% for each $E_{soil}$ increased by 100%, from 5 MPa to 10 MPa and from 10 MPa to 20 MPa. Hence, it is important to say in this study that $S_{sw}$ became half when the initial value $E_{soil}$ doubled.

Figure 14 shows contours heaving of square footing in soil mass with $E_{soil}$ variation and $\sigma_0$=300 kPa. A small 3D section in output results ($x$=$y$=5$m$, $z$ between 8.5 and 11$m$) was considered to show the contours of the heave. This was due to the importance of the area near the foundation. In all cases, the final heave was maximum at the soil mass surface, then it decreased with the depth. Moreover, it was observed that the value of the maximum amplitude of the heave vectors varied with the rigidity of the soil $E_{soil}$, for larger elastic modulus values, the maximum heave of the footing became smaller.

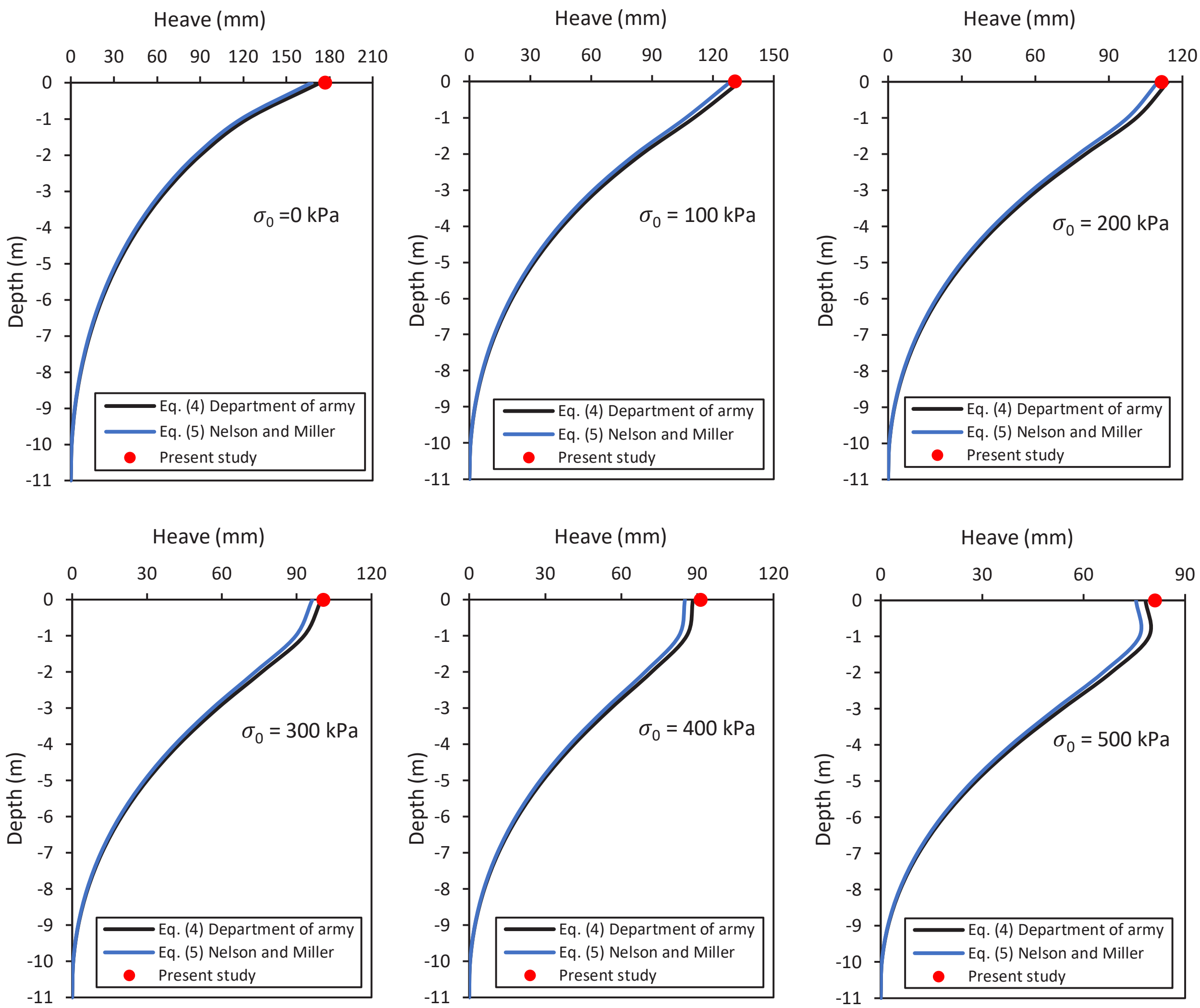


**Figure 10:** Comparison between numerical and analytical results of heave evolutions throughout the soil depth. Case of square footing of width B=1m and $\sigma_0$=0 to 500 kPa.

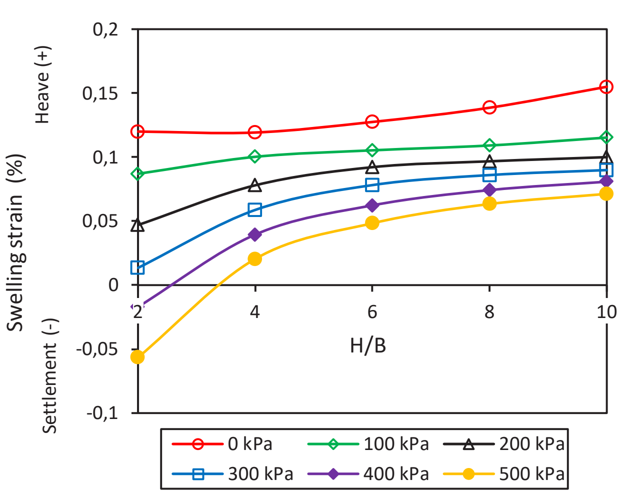


**Figure 11:** Variation of vertical swelling strain $\varepsilon_{sw}$ after swelling for square footing with *H/B* ratio and $\sigma_0$=0 to 500 kPa.

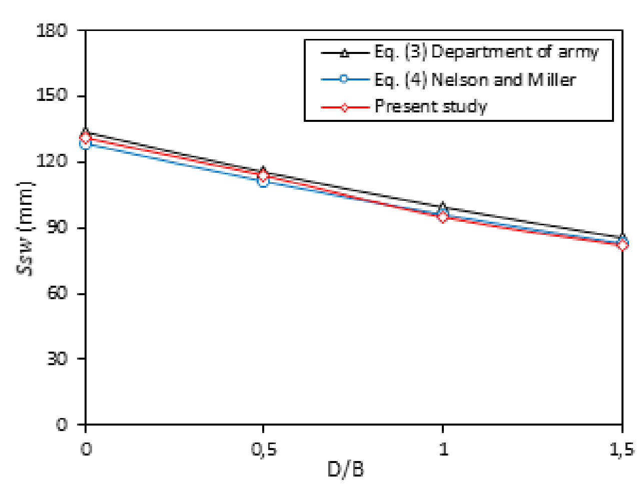


**Figure 12:** Comparison between numerical and analytical results of square footing heave $S_{sw}$ with *D/B* ratio for $\sigma_0$= 100 kPa.

# 6 Conclusions

In this paper, a series of numerical analysis by finite-difference code FLAC were performed for isolated shallow foundations, subjected to a distributed vertical loading founded on a saturated swelling clayey soil mass following the Mohr–Coulomb (MC) failure criterion. We confirmed that the numerical computation results of the footing heave were compatible with the analytical predictions based on oedometer tests proposed in the literature. Based on the results of this numerical and analytical study, important conclusions drawn from this work include:

– The proposed numerical model based on the simulation of the swelling pressure is able to predict the heave of the soil mass loaded by a shallow foundation.

– Numerical analyses show that the swelling strain $\varepsilon_{sw}$ of the footing to a non-linear form increases with the increase of the swelling layer thickness $H/B$. A settlement strain of the footing can occur when $H/B$ is very small and the applied loads are very large.

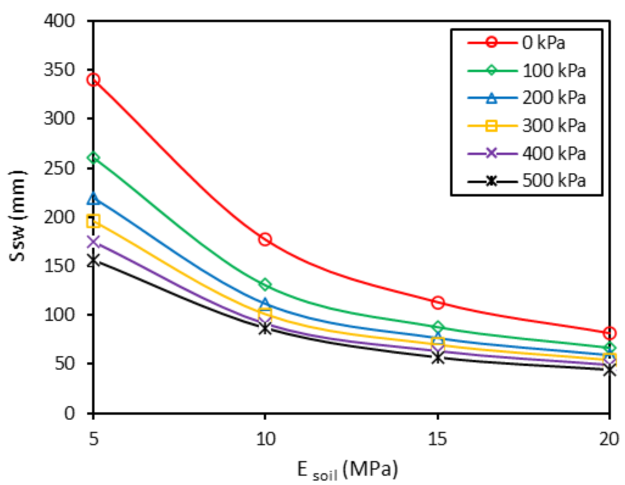


**Figure 13:** Variation of square footing heave $S_{sw}$ of width B=1m with soil stiffness $E_{soil}$ for $\sigma_0$=0 to 500 kPa.

**Table 4:** Heave prediction analytical and numerical of rectangular and circular footing with *D/B* ratio for $\sigma_0$= 100 kPa.

| *D/B* | $S_{sw}$ (mm) Rectangular footing | | | $S_{sw}$ (mm) Circular footing | | |
|---|---|---|---|---|---|---|
| | Present study | Department of army | Nelson And Miller | Present study | Department of army | Nelson And Miller |
| 0 | 125.2 | 125.7 | 121.3 | 125.1 | 135.4 | 130.6 |
| 0.5 | 116.1 | 108.6 | 104.8 | 114.3 | 116.8 | 112.7 |
| 1.0 | 100.4 | 93.6 | 90.2 | 99.3 | 100.7 | 97.1 |
| 1.5 | 88.5 | 80.4 | 77.5 | 87.4 | 86.6 | 83.5 |

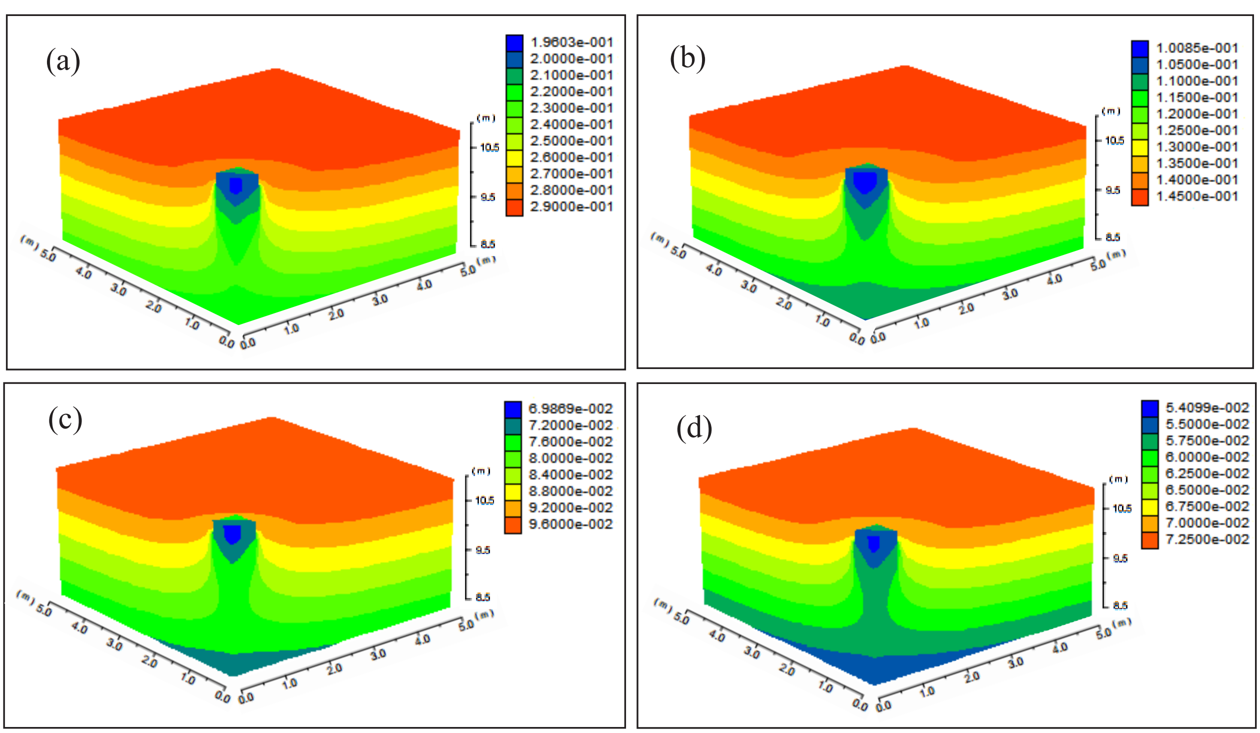


**Figure 14:** Contours heaving of square footing of width B=1m and $\sigma_0$=300 kPa with $E_{soil}$ variation: (a) $E_{soil}$=5 MPa, (b) $E_{soil}$=10 MPa, (c) $E_{soil}$=15 MPa, (d) $E_{soil}$=20 MPa.

- In case of an equality between the applied load $\sigma_0$ and the swelling pressure $\sigma_{sw}$, this doesn't mean a lack of heaving of the footing $S_{sw}$. It only characterizes the nullity of the swelling strain at depth $z_i$ of the soil mass.
- The embedment of the footing has influence on the total heave, a linear decrease in heave $S_{sw}$ was observed with an increase in the $D/B$ ratio.
- It can be stated that when the soil stiffens due to the increase in $E_{soil}$, the final heave of the footing $S_{sw}$ becomes smaller, which indicates the important influence of this parameter.

## References

[1] Nelson, J.D., Miller, D.J. (1992). Expansive soils: problems and practice in foundation and pavement engineering. J. Wiley, New York.

[2] Nelson, J.D., Chao, K.C., Overton, D.D., Nelson, E.J. (2015). Foundation engineering for expansive soils. Wiley, Hoboken, New Jersey.

[3] Chen, F.H. (1975). Foundations on expansive soils. Elsevier Scientific Pub. Co, Amsterdam; New York.

[4] Fredlund, D.G., Rahardjo, H., Fredlund, M.D. (2012). Unsaturated soil mechanics in engineering practice. Wiley, Hoboken, NJ.

[5] Tang, A.M., Cui, Y.J., Trinh, V.N., Szerman, Y., Marchadier, G. (2009). Analysis of the railway heave induced by soil swelling at a site in southern France. *Engineering Geology*. 106 (1), 68–77.

[6] Hachichi, A., Fleureau, J.M. (1999). Caractérisation et stabilisation de quelques sols gonflants d'Algérie. *Revue Française de Géotechnique*. 86 37–51.

[7] Djedid, A., Bekkouche, A., Aissa Mamoune, S.M. (2001). Identification and prediction of the swelling behaviour of some soils from the Tlemcen region of Algeria. *Bulletin Des Laboratoires Des Ponts et Chaussées 4375*. 233 69–77.

[8] Medjnoun, A., Khiatine, M., Bahar, R. (2014). Caractérisation minéralogique et géotechnique des argiles marneuses gonflantes de la région de Médéa, Algérie. *Bulletin of Engineering Geology and the Environment*. 73 (4), 1259–1272.

[9] Adem, H.H., Vanapalli, S.K. (2015). Review of methods for predicting in situ volume change movement of expansive soil over time. *Journal of Rock Mechanics and Geotechnical Engineering*. 7 (1), 73–86.

[10] Magnan, J.P., Ejjaaouani, H., Shakhirev, V., Bensallam, S. (2013). Etude du gonflement et du retrait d'une argile. *Bulletin Des Laboratoires Des Ponts et Chaussées*. 155–170.

[11] Mitchell, P.W., Avalle, D.L. (1984). A technique to predict expansive soils movement. in: Proc. 5th Int. Conf. Expans. Soils, Adelaide, Australia, pp. 124–130.

[12] Mckeen, R.G. (1992). A model for predicting expansive soil behavior. in: Proc. 7th Int. Conf. Expans. Soils, Dallas-Texas, pp. 1–6.

[13] Fityus, S., Smith, D.W. (1998). A simple model for the prediction of free surface movements in swelling clay profiles. in: Proc. 2nd Int. Conf. Unsaturated Soil, Beijing, China, pp. 473–478.

[14] Briaud, J.L., Zhang, X., Moon, S. (2003). Shrinkage test – water content method for shrinkage and swell predictions. *Journal of Geotechnical and Geoenvironmental Engineering*. 129 (7), 590–600.

[15] Vanapalli, S.K., Lu, L., Oh, W.T. (2010). Estimation of swelling pressure and 1-D heave in expansive soils. in: Proc. 5th Int. Conf. Unsaturated Soils, Barcelona, Spain, pp. 1201–1207.

[16] Fredlund, D.G. (1983). Prediction of ground movements in swelling clays. in: Proc. 31st Annu. Soil Mech. Found Eng. Conf., Earle Brown Centre, University of Minnesota, Minneapolis, pp. 1–48.

[17] US Department of the Army (DA). (1983). Foundations in Expansive Soils. *Technical Manual TM 5-818-7*.

[18] Nelson, J.D., Reichler, D.K., Cumbers, J.M. (2006). Parameters for heave prediction by oedometer tests. in: Proc. 4th Int. Conf. Unsaturated Soils, Carefree, Arizona, pp. 951–961.

[19] Ejjaaouani, H., Shakhirev, V. (2007). Calculation of foundations during soil wetting. in: Proc. 14th Eur. Con. Soil Mech. Geo Eng, Madrid, Spain, pp. 727–731.

[20] Baheddi, M., Djafarov, M., Charif, A. (2016). A method for predicting the deformation of swelling clay soils and designing shallow foundations that are subjected to uplifting. *Acta Geotechnica Slovenica*. 13 (1), 67–77.

[21] Hung, Q.V., Fredlund, D.G. (2004). The prediction of one-, two-, and three-dimensional heave in expansive soils. *Canadian Geotechnical Journal*. 41 (4), 713–737.

[22] Masia, M.J., Totoev, Y.Z., Kleeman, P.W. (2004). Modeling Expansive Soil Movements beneath Structures. *Journal of Geotechnical and Geoenvironmental Engineering*. 130 (6), 572–579.

[23] Hung, Q.V., Fredlund, D.G. (2006). Challenges to modelling heave in expansive soils. *Canadian Geotechnical Journal*. 43 (12), 1249–1272.

[24] Abed, A.A. (2008). Numerical modeling of expansive soil behavior, PhD Thesis, Stuttgart University.

[25] Nowamooz, H., Mrad, M., Abdallah, A., Masrouri, F. (2009). Experimental and numerical studies of the hydromechanical behaviour of a natural unsaturated swelling soil. *Canadian Geotechnical Journal.* 46 (4), 393–410.

[26] ASTM D4546-08. (2008). Standard test methods for one-dimensional swell or settlement potential of cohesive soils. *West Conshohocken, PA*.

[27] Jahangir, E., Deck, O., Masrouri, F. (2012). Estimation of ground settlement beneath foundations due to shrinkage of clayey soils. *Canadian Geotechnical Journal*. 49 (7), 835–852.

[28] Holtz, R.D., Kovacs, W.D. (1981). An introduction to geotechnical engineering. Prentice-Hall, Englewood Cliffs, N.J.

[29] Vanapalli, S.K., Lu, L. (2012). A state-of-the art review of 1-D heave prediction methods for expansive soils. *International Journal of Geotechnical Engineering*. 6 (1), 15–41.

[30] Tang, C.S., Tang, A.M., Cui, Y.J., Delage, P., Schroeder, C., Laure, E.D. (2011). Investigating the Swelling Pressure of Compacted Crushed-Callovo-Oxfordian Claystone. *Physics and Chemistry of the Earth, Parts A/B/C*. 36 (17), 1857–1866.

[31] Wang, Q., Tang, A.M., Cui, Y.J., Delage, P., Gatmiri, B. (2012). Experimental study on the swelling behaviour of bentonite/claystone mixture. *Engineering Geology*. 124, 59–66.

[32] Saba, S., Cui, Y.J., Tang, A.M., Barnichon, J.D. (2014). Investigation of the swelling behaviour of compacted bentonite–sand mixture by mock-up tests. *Canadian Geotechnical Journal*. 51 (12), 1399–1412.
[33] Nelson, J.D., Overton, D.D., Durkee, D.B. (2001). Depth of Wetting and the Active Zone. in: Shal found and soil prop, ASCE. Civ Eng. Conf, Houston, Texas, United States, pp. 95–109.
[34] FLAC3D. (2003). Fast Lagrangian Analysis of Continua in 3 dimensions, Version 3.0. *ITASCA Consulting Group, Inc*.
[35] Kaliakin, V.N. (2017). Soil Mechanics: calculations, principles, and methods. Butterworth-Heinemann, an imprint of Elsevier, Kidlington, Oxford Cambridge.